Crystal and Electronic Structures and Linear Optics of Strontium Pyroborate

Q.-S. Lin, W.-D. Cheng,[1] J.-T. Chen, and J.-S. Huang[1]

Fujian Institute of Research on the Structure of Matter, Chinese Academy of Sciences, State Key Laboratory of Structural Chemistry, Fuzhou, Fujian 350002, People's Republic of China

The compound $Sr_2B_2O_5$ has been synthesized by high temperature solution reaction. It crystallizes in the monoclinic space group $P2_1/c$ with cell dimensions $a = 7.719(4)$, $b = 5.341(1)$, $c = 11.873(2)$Å, $\beta = 92.71(2)°$, $V = 488.9(3)$ Å^3, and $Z = 4$, $D_{calc} = 3.76$ g/cm^3. The structure comprises SrO_7 and SrO_6 polyhedra and B_2O_5 groups. The electronic structure has been calculated by the INDO/S method for this compound, and the dynamic refractive indices have been obtained in terms of INDO/SCI following combination with the sum-over-states method. The calculated energy gap is 4.26 eV between the upper valence band and lower conduction band, and the calculated average refractive index is 1.791 at a wavelength of 1.065 μm. The charge transfers from O^{2-} anion orbitals to Sr^{2+} cation orbitals make the significant contributions to linear polarizability in terms of analyses of atomic state density contributing to the valence and conduction bands. © 1999 Academic Press

INTRODUCTION

The SrO—B_2O_3 system has been studied extensively since it was reported that there are five compounds (3:1, 2:1, 1:1, 1:2, 1:3) in this system (1–5). The phase equilibrium diagram was determined using the DTA technique (6). The luminescence of tetraborate SrB_4O_7 was studied (7, 8) and the single crystal structure of SrB_2O_4 was determined (9). Powder diffraction analyses of $Sr_2B_2O_5$ has also been done (10). In recent years, strontium borate has become a focus of interest due to the possibility of it being a new nonlinear optical material. In this paper, we report the synthesis of $Sr_2B_2O_5$ in high temperature solution reaction and the determination of its crystal structure by single-crystal X-ray diffraction techniques. We also report the calculated electronic structure and linear polarizability of microspecies $Sr_2B_2O_5$ and calculated refractive index of bulk $Sr_2B_2O_5$. It is found that the charge transfers from the oxygen atomic

orbital to strontium atomic orbital make the significant contributions to the polarizability.

EXPERIMENTAL AND COMPUTATIONAL PROCEDURES

Preparation

Crystals of the title compound were grown from a mixture containing appropriate amounts of $SrCO_3$ (chemically pure), KFB_4 (chemically pure), and H_3BO_3 (analytical reagent). The mixture was thoroughly milled, heated in a platinum crucible in air to 1193 K, and kept at 1193 K for 15 h. The temperature was quickly quenched to 1053 K and slowly cooled from 1053 to 973 K at a rate of 0.011 K/h and then air quenched to room temperature. Colorless crystals were obtained.

X-Ray Determination

A crystal with approximate dimensions $0.38 \times 0.30 \times 0.10$ mm^3 was selected for single-crystal X-ray diffraction. The diffraction data are collected on an Enraf–Nonius CAD4 diffractmeter with graphite monochrometer Mo$K\alpha$ radiation ($\lambda = 0.71073$ Å). Cell constants were obtained from least-squares refinement, using the setting angles of 23 reflections in the range $11° < \theta < 18°$. The cell parameters and calculated volume are: $a = 7.719(4)$, $b = 5.341(1)$, $c = 11.873(2)$ Å, $\beta = 92.71(2)°$, $V = 488.9(3)$ Å^3, $Z = 4$, F.W. = 276.86, and Dm = 3.76 g/cm^3. The data were collected at 273 K using the $\omega/2\theta$ scan technique with a scan speed 5°/min and a scan width $\Delta\omega = (0.8 + 0.35 \tan\theta)°$. The intensities of three standard reflections were measured every 60 min and the indensity decay was 3.9%. Lorentz and polarization corrections were applied to the data. The linear absorption coefficient is 210.9 cm^{-1}. An empirical absorption correction based on ψ-scan was applied and the relative transmission coefficients ranged from 0.490 to 0.997 with an average value of 0.752. The 3340 reflections were used to measure with $2\theta = 80°$; 1734 reflections

TABLE 1
Fractional Atomic Coordinates and Equivalent Isotropic Displacement Parameters (Å)

Atom	x	y	z	U_{eq}[a]
Sr(1)	0.62319(9)	0.4098(1)	0.34069(5)	0.0088(1)
Sr(2)	1.11767(9)	0.4502(1)	0.36749(5)	0.0092(1)
O(1)	0.3571(7)	0.151(1)	0.3517(4)	0.012(1)
O(2)	0.6071(7)	0.212(1)	0.1404(4)	0.014(1)
O(3)	0.9013(7)	0.092(1)	0.3313(4)	0.013(1)
O(4)	0.8537(7)	0.698(1)	0.4279(4)	0.012(1)
O(5)	0.7463(7)	0.101(1)	0.4927(4)	0.015(1)
B(1)	0.660(1)	0.068(2)	0.5950(6)	0.010(1)
B(2)	0.839(1)	−0.047(2)	0.4159(6)	0.010(1)

[a] $U_{eq} = (1/3)\sum_i\sum_j U^{ij}\alpha_i^*\alpha_j^* a_i a_j$.

with $I > 3\sigma(I)$ were used in structural determination and refinement.

The structure was determined by the Mo1EN/PC program. From the systematic absence of $h01: 1 = 2n$; $0k0: k = 2n$ and from subsequent least-squares refinement, the space groups was determined to be $P2_1/c(\#14)$. The strontium atoms were located from the E-map; the remaining atoms were located in succeeding difference Fourier synthesis. The final full-matrix least-squares refinement for 82 variable parameters converged to $R = 5.98\%$, $R_w = 5.94\%$ [$W = 1/\sigma^2(F)$], $S = 1.37$, $(\Delta/\sigma)_{max} = 0.0003$; neutral atomic scattering factors were taken from Cromer and Waber (11). The maximum and minimum peaks on the final different Fourier map are 3.93 and $-0.96\,e/\text{Å}^3$, respectively. The atoms coordinations and thermal parameters are listed in Table 1.

Computational Details

Some of the obtained results from electronic structural calculation were employed to compute microscopic polarizability, and the electronic structural calculations of the isolated molecules (microspecies of the title compound) were based on an all-valence-electron, semi-empirical INDO self-consistent field (SCF) molecular orbital (MO) procedure with configuration interaction (CI) modified by Zerner and co-workers (12–15). There are the one-center core integral $U_{\mu\mu}$, resonance integral $\beta_{\mu\nu}$, two-electron integral $\gamma_{\mu\nu}$, overlap integral $S_{\mu\nu}$, and density matrix element $P_{\mu\nu}$ in the matrix element of the Fock operator under the INDO approximation. The INDO model as employed herein included all one-center, two-electron integrals and two-center, two-electron integrals $\gamma_{\mu\nu}$. The one-center two-electron integrals $\gamma_{\mu\mu}$ were chosen from the Pariser approximation (16), $\gamma_{\mu\mu} = F^0(\mu\mu) = IP_\mu - EA_\mu$, and the two-center two electron integrals were calculated using the Mataga–Nishimoto formula (17), $\gamma_{\mu\nu} = 1.2/[R_{AB} + 2.4/(\gamma_{\mu\mu} + \gamma_{\nu\nu})]$ in the spectroscopic version of the INDO method. The Slater orbital

exponents ζ and the other calculation parameters are listed in ref. (18). The molecular orbital calculations were performed by the restricted Hartree–Fork method. The ground state, which was obtained from calculated results of the SCF, was taken as the reference state in the CI. Only single-substituted determinants relative to the ground state configuration were considered and only singlet spin-adapted configurations needed to be included in the CI calculations. The ground state and all excited states had the multiplicity of one. The electron was promoted from the thirteen highest occupied orbitals to the thirteen lowest unoccupied orbitals and the configuration space was constructed by these 26 active orbitals. The wavefunctions and energy eigenvalues of the excited states were determined by solving the secular equation relating to configuration coefficients. The dipole and transition moment matrix elements were expressed as a sum of one-electron integrals.

The tensor components of the polarizability $\alpha(\omega)$ with frequency dependence for the microspecies of the title compound was calculated by the sum-over-states (SOS) method as follows:

$$\alpha_{ij}(\omega) = 1/\hbar\sum_m \mu_{gm}^i \mu_{mg}^j [(\omega_{mg} - \omega_p)^{-1} + (\omega_{mg} + \omega_p)^{-1}]. \quad [1]$$

The molecular configuration of the microspecies was based on crystallographic data, and the electronic structures and susceptibilities were calculated using this empirical structure.

RESULTS AND DISCUSSIONS

Crystal Structure

The structure is based on Sr_4O_{19} tetramers and it was composed of two $Sr(1)O_7$ and two $Sr(2)O_6$ polyhedra. These two polyhedra link by four shared $O\cdots O$ edges to form a double-chain extending along the a direction. The double-chains link together to form sheets parallel to the ac plane by sharing O(4) atoms. These sheets stack along the b direction to form the three-dimensional framework by sharing O(1), O(2), and O(3) atoms. The $[B_2O_5]$ group bridges the adjacent double-chains and adjacent sheets together. A similar structure to the title compound is $Mg_2B_2O_5$ (19). It is built from the Mg_4O_{18} tetramer sharing three edges and connected by the B atom to form chains extending along $[0\,1\,0]$. However, the tetramer itself is discrete and forms an infinite chain only by B atoms.

Figure 1 shows the structure of monoclinic $Sr_2B_2O_5$. In this crystal, Sr atoms have different coordination environments; that is, Sr(1) atoms are coordinated by seven O atoms while Sr(2) atoms are coordinated by six O atoms. The $Sr(1)O_7$ polyhedron may be described as a monocapped distorted triangular prism. The Sr(1)–O distances vary from 2.418(6) to 2.743(6) Å with an average value of 2.572 Å, which compared well to the expected value 2.59 Å calculated
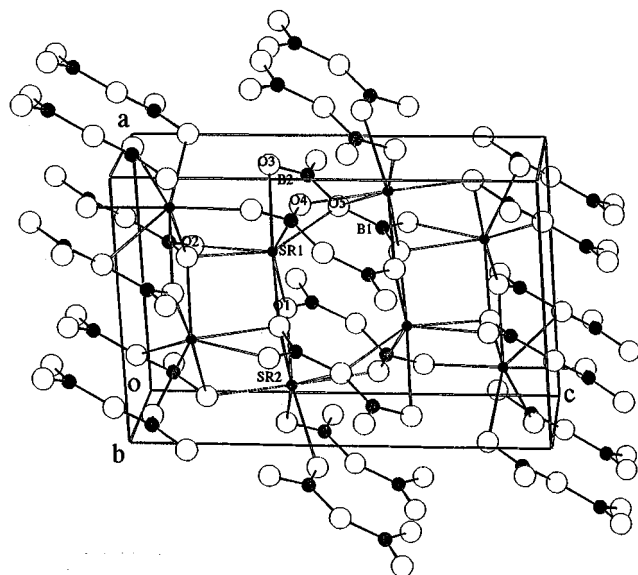
FIGURE 1

Bond	Dist. (Å)	Angle	(°)
Sr(1)–O(1)	2.485(5)	O(1)–Sr(1)–O(2)	79.5(2)
Sr(1)–O(1)	2.632(5)	O(1)–Sr(1)–O(5)	83.4(2)
Sr(1)–O(2)	2.600(5)	O(2)–Sr(1)–O(3)	73.4(2)
Sr(1)–O(2)	2.418(6)	O(2)–Sr(1)–O(5)	112.2(2)
Sr(1)–O(3)	2.743(6)	O(3)–Sr(1)–O(4)	081.8(2)
Sr(1)–O(4)	2.537(5)	O(3)–Sr(1)–O(5)	051.2(2)
Sr(1)–O(5)	2.590(5)	O(4)–Sr(1)–O(5)	082.8(2)
Sr(2)–O(1)	2.458(5)	O(1)–Sr(2)–O(2)	073.9(2)
Sr(2)–O(2)	2.548(5)	O(1)–Sr(2)–O(3)	097.9(2)
Sr(2)–O(3)	2.563(6)	O(1)–Sr(2)–O(4)	165.7(2)
Sr(2)–O(3)	2.476(5)	O(2)–Sr(2)–O(3)	079.0(2)
Sr(2)–O(4)	2.561(5)	O(2)–Sr(2)–O(4)	113.8(2)
Sr(2)–O(4)	2.554(5)	O(3)–Sr(2)–O(4)	087.4(2)
B(1)–O(1)	1.340(9)	O(1)–B(1)–O(2)	121.8(6)
B(1)–O(2)	1.36(1)	O(1)–B(1)–O(5)	124.9(7)
B(1)–O(5)	1.423(9)	O(2)–B(1)–O(5)	113.1(6)
B(2)–O(3)	1.358(9)	O(3)–B(2)–O(4)	126.1(6)
B(2)–O(4)	1.37(1)	O(3)–B(2)–O(5)	111.9(6)
B(2)–O(5)	1.426(9)	O(4)–B(2)–O(5)	121.9(6)

from the crystal radii for the seven-coordinate Sr^{2+} ion (20). The $Sr(2)O_6$ polyhedron is a distorted octahedron with Sr(2)–O distances varying from 2.458(5) to 2.563(6) Å. The $[B_2O_5]$ group shows an interest for its coordinate manner. It can be viewed as a unidentate or a bidentate connection with the Sr atom. This case is the same as the $[B_2O_5]$ groups in $BaCuB_2O_5$ (21a). However, as far as the bidentation is concerned in $Sr_2B_2O_5$, the anticipated dentate atoms are different (Fig. 2). Three $[B_2O_5]$ groups are connected to the Sr(1) atom in a unidentate manner and two groups in a bidentate manner. The dentate atoms are O(1), O(2) and O(3), O(5), respectively, whereas there are four unidentate
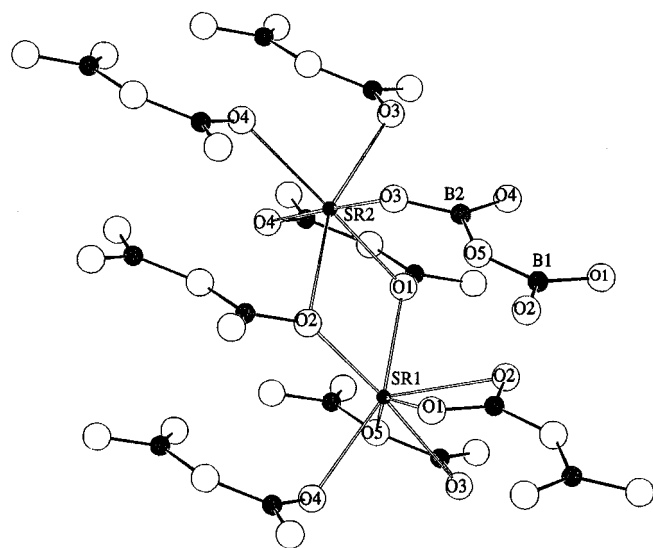
and one bidentate $[B_2O_5]$ groups with dentate atoms O(1), O(4) to the Sr(2) atom. The B–O–B angle in double-triangle $[B_2O_5]$ group is 138.1° and the two traingles derivate from planarity by approximately 3.7°. These angle degrees are small differences from the values found in the powder diffraction analyses of $Sr_2B_2O_5$ (10); however, these values do fall within the reported ranges of B–O–B angles, 112° ~ 180°, and interplanar angles, 0° ~ 76.8° in pyroborate compounds (21b). As can be seen in Table 2, the bond distances between the terminal O and B atoms are shorter than those between the bridging atom O(5) and B atom. This is due to the fact that the terminal O atom is bonding only to one B atom, while the bridge atom O(5) is bonding to two B atoms and weakens the B–O(5) bonds. Expect that the O(5) atom is bonding to two B atoms and one Sr atom, the other O atoms are bonding to three Sr atoms and one B atom in a distorted tetrahedral arrangement.

Electronic Structures

The calculations of electronic structures are based on the INDO/S quantum chemical method. The special molecular cluster using in the calculations is $Sr_2B_2O_5$, in which the molecular configuration is a double-triangle $[B_2O_5]$ group with B–O–B angle of 138° and one of two terminal O atoms in each triangle connecting one Sr atom. The calculated energy bands are divided into four zones for the $Sr_2B_2O_5$ and the topmost level in the valence band is regarded as a reference in order for convenience of descriptions. The zone of energy between −22.1 and −27.8 eV is a lower
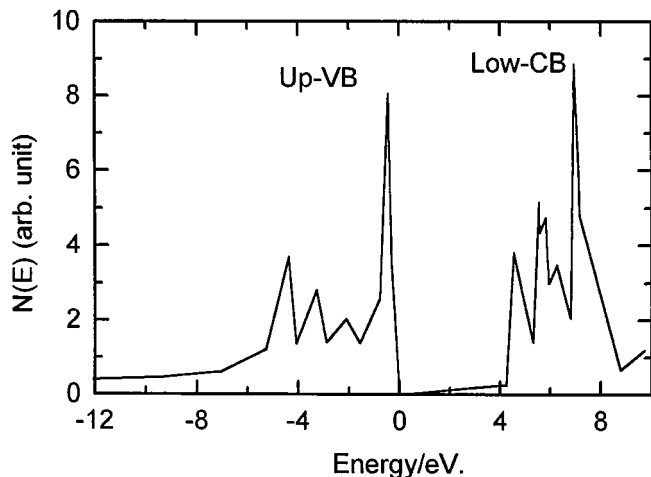

FIGURE 2

FIG. 3. State density.

valence band and this zone is attributable to the 2s orbitals of the oxygen and boron atoms. There are $77 \sim 85\%$ O–2s and less than 7% B–2s orbital characters in this zone. It is approximately assigned as an s valence band. The second zone from -12.1 to 0.00 eV is a contribution from the $49 \sim 97\%$ O–2p orbital character, but mixing with $< 20\%$ B–2p orbital character, and it is an upper valence band zone. These two band zones are fully occupied by electrons. The closer the top edge of valence band (VB), the more contributions are from the O–2p orbitals. The atomic state density of the upper VB zone, i.e., the calculated second zone, is displayed in Fig. 3. It is found that the band between the -12.1 and -5.3 eV is the contribution from σ-bonding interactions between the O–2p and B–2p orbitals. The three peaks localized in the energies $-5.2 \sim -1.6$ eV can be assigned as the π-bonding interactions between the O–2p and B–2p orbitals. For example, the peak in the energy at about -4.38 eV consists of 72% O p_z and 14% B p_z orbitals. The peak localized in the energies $-1.5 \sim 0.0$ eV is assigned as the 2p nonbonding orbitals of the oxygen atoms (O–2p orbital contributions of $> 94\%$). The third zone is a lower conduction band (CB) and its atomic state density is shown on the right side of Fig. 3. The peaks localized in the energy region between 4.3 and 7.2 eV are all the contributions from the strontium ionic state ($>90\%$). The three peaks from the left to right in the CB, as shown in Fig. 3, are, in turn, contributions from the Sr 5s ($\approx 91\%$), 4d ($75\% \sim 100\%$), and 5p ($\approx 95\%$) states. The fourth zone from 8.7 to 21.6 eV is made up of the antibonding interactions between the boron and oxygen atomic valence orbitals. The last two zones are completely empty ones. It is noted that these assignments for atomic states are only a general trend. From Fig. 3, it is found that the calculated energy gap between the upper VB and lower CB is 4.26 eV. The UV absorption edge of $Sr_2B_2O_5$ crystal will be estimated to be about 290 nm from this gap.

Optical Properties

Optical properties of bulk can be thought of as being built up from the corresponding properties of individual molecule or microscopic species, and the susceptibility of bulk has a relation with the polarizability of microspecies. Therefore, linear susceptibility of the bulk can be calculated using the given linear polarizability of microspecies. The linear refractive index of frequency dependence can be written in the standard manner, that is, by

$$n^2(\omega) = 1 + 4\pi\chi^{(1)}(\omega), \qquad [2]$$

in which the linear susceptibility $\chi^{(1)}(\omega)$ is defined as

$$\chi^{(1)}(\omega) = N\alpha(\omega)/[1 - (4\pi/3)N\alpha(\omega)]. \qquad [3]$$

Here, $\alpha(\omega)$ is the frequency dependent polarizability which obtained by Eq. [1], and N is the molecular number density. The practical form of N is obtained by the product of mass density and Avogadro's constant dividing by molar mass. For $Sr_2B_2O_5$, with a molecular formula weight of 276.86 g/mol and a mass density of 3.76 g/cm³, we obtain $N = 8.179 \times 10^{21}$ cm^{-3}. Before attempting to compute the variation of the refractive index against wavelengths for the bulk $Sr_2B_2O_5$, it is necessary to investigate the behavior of the convergence in the summation of excited states and check if the results calculated from the INDO/SCI method are reliable. Figure 4 shows the plots of the calculated average polarizability $\langle\alpha\rangle$ versus the number of states for the microspecies of the title compound at the wavelength 1064 nm. Although the convergence is slow, the line is stable after summation over 150 states. From analyses combining Fig. 4 with the states contributing to polarizability, we can find that the polarizabilities are mainly contributions from charge transfers from the O–2p to Sr–5s orbital for the states below state 71 and charge transfers from the O–2p to Sr–4d or –5p orbital for the states at or up to state 72, and charge transfers make larger contributions to the polarizability
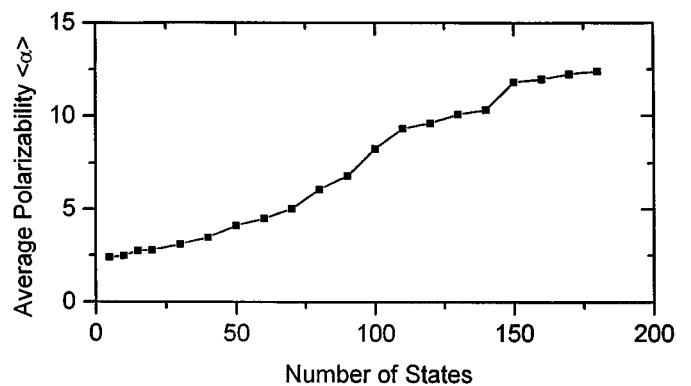
FIG. 4. The polarizability $\langle\alpha\rangle$ of microspecies at $\lambda = 1064$ nm.
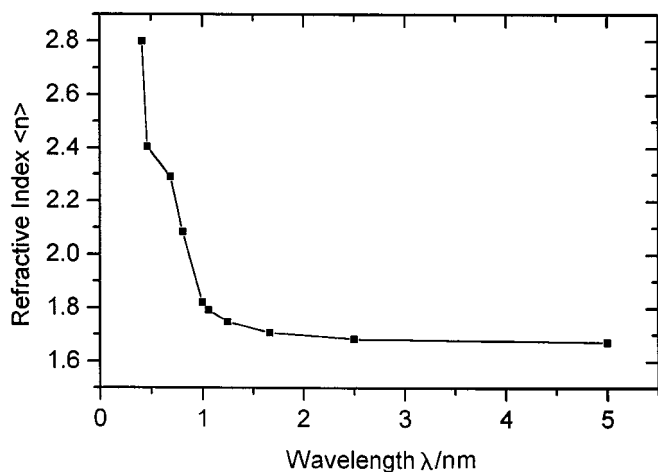
FIG. 5. The calculated dynamic refractive index $\langle n(\omega) \rangle$.

from the latter than from the former cases. For instance, the fourth state and the 70th state have the greatest contributions from the 64% configuration, $\phi_{20 \to 22}$, and the 52% configuration, $\phi_{13 \to 21}$, respectively. The configuration $\phi_{20 \to 22}$ is formed by an electron from the φ_{20} molecular orbital (MO) composed of 97% O–2p orbital to the φ_{22} MO composed of 91% Sr–5s orbital, and the configuration $\phi_{13 \to 21}$ is formed by an electron from the φ_{13} MO composed of 87% O–2p orbital to the φ_{21} MO composed of 92% Sr–5s orbital. The 72nd state has the major contributions from the configurations $\phi_{16 \to 30}$ (15%) and $\phi_{17 \to 32}$ (40%), and the 145th state has the major contributions from the configurations $\phi_{10 \to 25}$ (23%) and $\phi_{11 \to 32}$ (31%). The configuration $\phi_{17 \to 32}$ is formed by an electron from the φ_{17} MO composed of 94% O–2p orbital to the φ_{32} MO composed of 75% Sr–4d and 17% Sr–5p orbitals, and the configuration $\phi_{10 \to 25}$ is formed by an electron from the φ_{10} MO composed of 72% O–2p and 15% B–2p orbitals, to the φ_{25} MO composed of 96% Sr–4d orbitals.

The average dynamic refractive index of $\langle n(\omega) \rangle$ is calculated by Eqs. [2] and [3] using a given average polarizability $\langle a \rangle = (a_{xx} + a_{yy} + a_{zz})/3$. The refractive index $\langle n(\omega) \rangle$ of bulk $Sr_2B_2O_5$ from the wavelengths of 0.40 to 5.00 μm have been calculated and plotted in Fig. 5. The refractive index of the $Sr_5B_2O_5$ crystal has not been observed, and the calculated results only compare with the homolog $Mg_2B_2O_5$. The observed refractive index, n_x, n_y, n_z is individually 1.589, 1.660, 1.674 and the average refractive index is 1.641 for the $Mg_2B_2O_5$ crystal (22); the calculated refractive index, n_x, n_y, n_z is individually 1.405, 1.812, 2.157, and

the average $\langle n(\omega) \rangle$ is about 1.791 at a wavelength of 1.065 μm for $Sr_2B_2O_5$ bulk. Therefore, the calculated average refractive index of $Sr_2B_2O_5$ bulk at a low frequency region seems reasonable.

ACKNOWLEDGMENTS

REFERENCES

1. P. B. Hart and S. E. F. Smallwood, *J. Inorg. Nucl. Chem.* **24**, 1047 (1962).
2. Krogh-Moe, *Acta Chem. Scand.* **18**, 2055 (1964).
3. C. E. Weir and R. A. Schroeder, *J. Res. Natlbur. Stand. Sect. A* **68**, 465 (1964).
4. S. Block, A. Perloff, and C. E. Weir, *Acta Cryst.* **17**, 314 (1964).
5. T. Koskentalo, M. Lesklä, and L. Niinistö, *Mater. Res. Bull.* **20**, 265 (1985).
6. H. Witzmann and G. Herzog, *Z. Phys. Chem.* **225**, 197 (1964).
7. A. Meijerink, J. Nuyten, and G. Blasse, *J. Lumin.* **44**, 19 (1989).
8. G. Blasse, G. J. Dirksen, and A. Meijerink, *Chem. Phys. Lett.* **167**, 41 (1990).
9. J. -B. Kim, K. -S. Lee, I. -H. Sun, J. -H. Lee, J. -R. Park, and Y. -H. Shin, *Acta Cryst. C* **52**, 498 (1996).
10. H. Bartl and W. Schuckmann, *Neues Jaharb. Mineral. Monatsh.* **8**, 253 (1966).
11. D. T. Cromer and J. T. Waber, *in* "International Tables for X-ray Crystallography," Vol IV, Table 2.2A, p. 71. Kynoch Press, Birmingham, 1974.
12. A. D. Bacon and M. C. Zerner, *Theoret. Chim. Acta* **53**, 21 (1979).
13. M. C. Zerner, G. H. Lovw, R. F. Kirchner, and U. T. Mueller-Westerhoff, *J. Am. Chem. Soc.* **102**, 589 (1980).
14. W. P. Anderson, E. D. Edwards, and M. C. Zerner, *Inorg. Chem.* **25**, 2728 (1986).
15. W. P. Anderson, T. R. Cundari, and M. C. Zerner, *Int. J. Quantum Chem.* **39**, 31 (1991).
16. R. Pariser, *J. Chem. Phys.* **21**, 568 (1953).
17. N. Motaga and K. Nishimoto, *Z. Phys. Chem.* **13**, 140 (1957).
18. The input parameters are as follows: Slater exponents Sr: $\zeta_{5s,5p} = 1.214 \text{ Å}^{-1}$, $\zeta_{4d,} = 2.058 \text{ Å}^{-1}$; B: $\zeta_{2s,2p} = 1.300 \text{ Å}^{-1}$, O: $\zeta_{2s,2p} = 2.275 \text{ Å}^{-1}$; valence state ionization energies Sr: $I_{5s} = -5.84 \text{ eV}$, $I_{5p} = -3.76 \text{ eV}$, $I_{4d} = -3.66 \text{ eV}$, B: $I_{2s} = -14.05 \text{ eV}$, $I_{2p} = -8.70 \text{ eV}$, O: $I_{2s} = -32.90 \text{ eV}$, $I_{2p} = -17.28 \text{ eV}$; Coulomb replusion integrals Ba: $\gamma_{5s5s} = \gamma_{5p5p} = \gamma_{5s5p} = 3.75 \text{ eV}$, $\gamma_{4d4d} = 5.31 \text{ eV}$, $\gamma_{4d5s} = \gamma_{4d5p} = 4.53 \text{ eV}$, B: $\gamma = 8.68 \text{ eV}$, O: $\gamma = 13.00 \text{ eV}$; resonance integrals Sr: $\beta_{5s} = \beta_{5p} = -1.88 \text{ eV}$, $\beta_{5d} = -10.05 \text{ eV}$, B: $\beta = -17.00 \text{ eV}$, O: $\beta = -34.20 \text{ eV}$.
19. G. -C. Guo, W. -D. Cheng, J. -T. Chen, H. -H. Zhang, J. -S. Huang, and Q.-E. Zhang, *Acta Crystallogr. C* **51**. 2469 (1995).
20. R. D. Shannon, *Acta Crystallogr. A* **32**, 751 (1976).
21. (a) R. W. Smith and D. A. Keszler, *J. Solid State Chem.* **129**, 184 (1997); (b) P. D. Thompson, J. Huang, R. W. Smith and D. A. Keszler, *J. Solid. State. Chem.* **95**, 126 (1991).
22. H. M. Davis and M. A. Knight, *J. Am. Ceram. Soc.* **28**, 97 (1945).